Intracranial Vessel Segmentation in 3D High-Resolution T1 Black-Blood MRI

S. Elsheikh, H. Urbach and M. Reisert

AJNR Am J Neuroradiol 2022, 43 (12) 1719-1721
doi: https://doi.org/10.3174/ajnr.A7700
http://www.ajnr.org/content/43/12/1719

Intracranial Vessel Segmentation in 3D High-Resolution T1 Black-Blood MRI

S. Elsheikh, H. Urbach, and M. Reisert

ABSTRACT

SUMMARY: We demonstrate the feasibility of intracranial vascular segmentation based on the hypointense signal in non-contrast-enhanced black-blood MR imaging using convolutional neural networks. We selected 37 cases. Qualitatively, we observed no degradation due to stent artifacts, a comparable recognition of an aneurysm recurrence with TOF-MRA, and consistent success in the differentiation of intracranial arteries and veins. False-positive and false-negative results were observed. Quantitatively, our model achieved a promising Dice similarity coefficient of 0.72.

ABBREVIATIONS: BBMRI = black-blood compressed-sensing MRI; CNN = convolutional neural networks; DSC = Dice similarity coefficient

Automated segmentation techniques of the cerebral vasculature are an area of interest, with numerous previous publications.[1] Currently, convolutional neural networks (CNN) are the criterion standard for medical image segmentation.[2] Publications applying CNN segmentation of the cerebral vessels were largely based on TOF-MRA.[3]

Recently, a black-blood compressed-sensing MRI (BBMRI) sequence was introduced. It allows isotropic voxels of 0.5 mm^3, suppression of signal within the vessels, and covering a large volume. These advantages are useful in diverse clinical applications.[4] We aimed to test the feasibility of intracranial vascular segmentation based on the hypointense signal in BBMRI using CNN.

Technical Report

After obtaining institutional review board approval, we retrospectively searched our PACS for examinations including BBMRI. We selected 37 (training, 26; testing, 11 randomly assigned [repeat examinations of the same patients were manually assigned to the training data set]) cases. The imaging indication was post-coiling examination in 34 cases, vasculitis in 2 cases, and dissection in 1 case.

All images were scanned on a 3T MR imaging (Magnetom Prisma; Siemens).[4] The image matrix was 384 × 384 × 256; voxel size, 0.55× 0.55× 0.6 mm^3.

We limited the volume of interest to cover the proximal course of the intracranial vessels and to extend beyond the circle of Willis (Online Supplemental Data). A binary mask was manually created in the Montreal Neurological Institute space (Online Supplemental Data) and then transformed to the individual patient space; this was used to define the cropped volume. Ground truth annotation was performed by a neuroradiologist (S.E.) with 15 years of experience in neurovascular imaging.

We used a hierarchic, multiscale, 3D CNN motivated by Yu et al.[5] Four scales of nested patches with a matrix size of 32^3 voxels were used. Scale sizes ranged from 105.6 × 105.6 × 76.8 mm^3 to 17.6 × 17.6 × 19.2 mm^3. The 2 intermediate scales were exponentially interpolated. The scales were randomly selected but with a 50% probability that the scale center lay within the target label. In each scale, a UNET-type architecture similar to that in Ronneberger et al[2] was used. The feature dimensions were 8, 16, 16, 32, 64. Max pooling in the encoding layers and transposed convolutions in the decoding layers were used. The input to the network was the BBMRI contrast normalized by the global signal mean. The output channels of each scale were forwarded as the input to the next scale (Online Supplemental Data). We trained the network using the Adam optimizer,[6] with a rate of 0.001 and binary cross-entropy. The network application used a random patching scheme, in which in each layer, only the highest probability (50%) daughter patches were further processed (https://bitbucket.org/reisert/patchwork/).

For evaluation of our test results, we measured the overlap and spatial distance metrics[7,8] using the Deepmind library (https://github.com/deepmind/surface-distance).

Received January 21, 2022; accepted after revision October 5.

From the Departments of Neuroradiology (S.E., H.U.) and Medical Physics, Functional Neurosurgery, and Stereotaxy (M.R.), Faculty of Medicine, Medical Center–University of Freiburg, Freiburg, Germany.

Please address correspondence to Samer Elsheikh, MD, Department of Neuroradiology, Breisacherstr 64, 79106 Freiburg im Breisgau, Germany; e-mail: samer.elsheikh@uniklinik-freiburg.de; @samerelsheikh

Indicates article with online supplemental data.

http://dx.doi.org/10.3174/ajnr.A7700

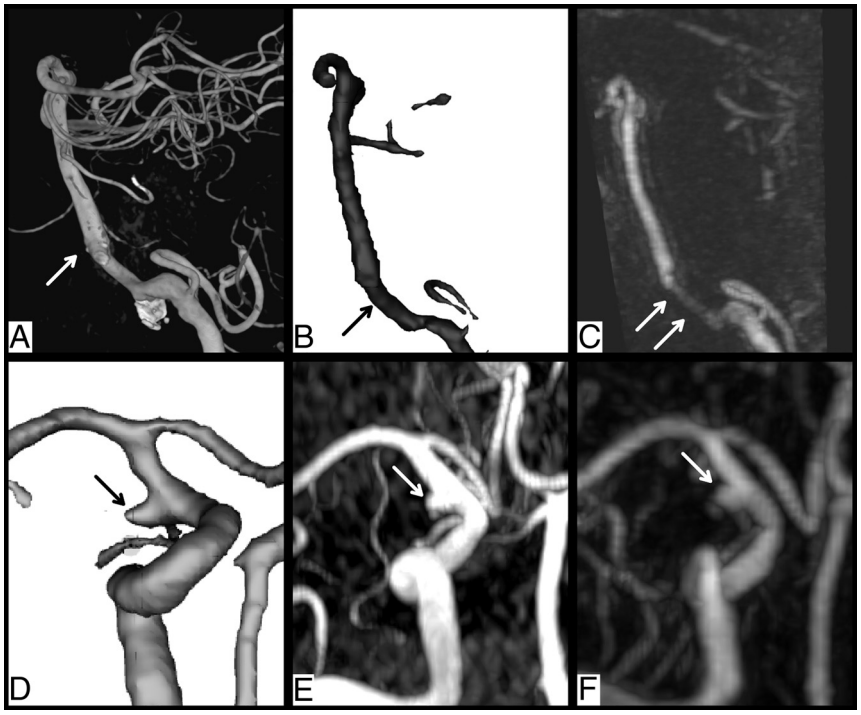

FIG 1. Sample images of advantageous findings. Identification of the vessel lumen following stent placement during treatment of a ruptured, dissecting aneurysm of the right vertebral artery in a test subject. *A*, 3D-rendering of rotational DSA in a lateral oblique projection following stent-assisted coiling (*arrow*, distal stent markers). *B*, Volume-rendering of the BBMRI model prediction (*arrow*, vessel lumen within the stent). *C*, Contrast-enhanced MRA shows partial signal degradation within the stent (*arrows*). *D–F*, Correct identification of a small recurrence (*arrows*) 6 months following coiling of a ruptured right posterior communicating artery aneurysm in a test subject. Volume-rendering in a coronal, oblique view of the BBMRI model prediction (*D*), of the TOF-MRA (*E*), and of the contrast medium–enhanced MRA (*F*).

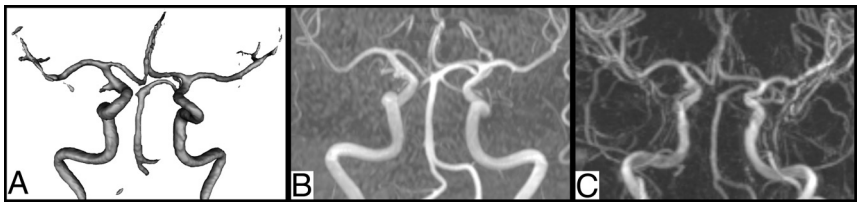

FIG 2. Anterior-posterior 3D-rendering of the intracranial vessel tree. *A*, BBMRI model prediction. *B*, TOF-MRA. *C*, Contrast-enhanced MRA.

Illustrative Findings in Testing Data Set

Segmentation of the vessel lumen following stent-assisted coiling of a ruptured dissecting aneurysm of the right vertebral artery was possible. The corresponding contrast-enhanced MRA showed signal degradation in the corresponding segment (Fig 1*A–C*). In another example, a small recurrence following coiling of a ruptured right posterior communicating artery aneurysm was successfully segmented. The segmentation was comparable with that in the TOF-MRA and the contrast-enhanced MRA (Fig 1*D–F*; overview, Fig 2). We observed a consistent true-positive and true-negative segmentation of intracranial arterial and venous structures in the volume of interest (Online Supplemental Data).

False-negative results were encountered in small-diameter vessels and in the distal vertebral arteries. They were rarely encountered in larger-diameter vessels. False-positive results were seen in areas showing low signal intensity in close proximity to the vessels, eg, metal artifacts following aneurysm clipping and in nearby bony structures (Online Supplemental Data).

Our model achieved Dice similarity coefficients (DSCs) of 0.77 and 0.72 in the training and testing data sets, respectively. The average evaluation metrics and corresponding plot are available in the Online Supplemental Data.

DISCUSSION

In this preliminary work, we demonstrate the feasibility of automated segmentation of the cerebral vasculature based on the negative contrast of the vessels in the non-contrast-enhanced BBMRI sequence. To our knowledge, this has not been previously attempted.

Qualitatively, vascular evaluation in the BBMRI is feasible. Differentiation between arterial and venous structures as well as recognition of morphologic changes (eg, aneurysm recurrence) were possible. Signal degradation following intracranial stent placement was not encountered (Fig 1 and Online Supplemental Data). The segmentation of smaller vessels and the distal vertebral arteries as well as the differentiation between vessels and nearby structures of low signal intensity (bony structures and aneurysm clips) were less accurate (Online Supplemental Data).

Quantitatively, our model achieved promising DSCs of 0.77 and of 0.72 in the training and testing data sets, respectively, indicating negligible overfitting. Our results are comparable with those of other TOF-based published works using CNN or thresholding techniques (DSC, 0.73–0.78). A more complex segmentation pipeline achieved a better DSC, reaching 0.93.[3,9,10]

A morphologic, flow-independent visualization of the cerebral vessels in the BBMRI has potential advantages. It avoids the flow-related artifacts and the stent-related signal degradation in TOF-MRA.[11,12] The large FOV and the high resolution[4] could allow segmentation of a large volume of interest. Furthermore, no application of contrast medium is required. Future prospects include further optimization of the machine learning parameters using a larger and more diverse data set, expanding the volume of interest, and testing performance in various intracranial pathologies.

CONCLUSIONS

CNN segmentation of the arteries of the circle of Willis and its branches in non-contrast-enhanced BBMRI with accuracy comparable with that of TOF-based segmentation techniques is feasible and promising.

Disclosure forms provided by the authors are available with the full text and PDF of this article at www.ajnr.org.

REFERENCES

1. Lesage D, Angelini ED, Bloch I, et al. **A review of 3D vessel lumen segmentation techniques: models, features and extraction schemes.** *Med Image Anal* 2009;13:819–45 CrossRef Medline
2. Ronneberger O, Fischer P, Brox T. **U-net: Convolutional networks for biomedical image segmentation.** In: Navab N, Hornegger J, Wells WM, et al, eds. *Medical Image Computing and Computer-Assisted Intervention–MICCAI 2015*. Springer; 2015:234–41
3. Cardoso MJ, Arbel T, Lee SL, et al, eds. *Intravascular Imaging and Computer Assisted Stenting, and Large-Scale Annotation of Biomedical Data and Expert Label Synthesis*. Springer; 2017 CrossRef
4. Guggenberger K, Krafft AJ, Ludwig U, et al. **High-resolution compressed-sensing T1 black-blood MRI.** *Clin Neuroradiol* 2021;31:207–16 CrossRef Medline
5. Xu Y, Gong M, Fu H, et al. **Multi-scale masked 3-D U-Net for brain tumor segmentation.** In: Xu Y, Gong M, Fu H, et al. *Brainlesion: Glioma, Multiple Sclerosis, Stroke and Traumatic Brain Injuries*. Springer; 2019:222–33 CrossRef
6. Kingma DP, Ba J. ***Adam: A Method for Stochastic Optimization.*** In: *Proceedings of the 3rd International Conference for Learning Representations*, San Diego, California. May 7–9, 2015
7. Taha AA, Hanbury A. **Metrics for evaluating 3D medical image segmentation: analysis, selection, and tool.** *BMC Med Imaging* 2015;15:29 CrossRef
8. Yeghiazaryan V, Voiculescu I. **Family of boundary overlap metrics for the evaluation of medical image segmentation.** *J Med Imaging (Bellingham)* 2018;5:015006 CrossRef Medline
9. Chen L, Xie Y, Sun J, et al. **3D intracranial artery segmentation using a convolutional autoencoder.** In: *Proceedings of the 2017 IEEE International Conference on Bioinformatics and Biomedicine (BIBM)*, Kansas City, Kansas. November 13–16, 2017 CrossRef
10. Zhang B, Liu S, Zhou S, et al. **Cerebrovascular segmentation from TOF-MRA using model- and data-driven method via sparse labels.** *Neurocomputing* 2020;380:162–79 CrossRef
11. Özsarlak Ö, Van Goethem JW, Maes M, et al. **MR angiography of the intracranial vessels: technical aspects and clinical applications.** *Neuroradiology* 2004;46:955–72 CrossRef Medline
12. Marciano D, Soize S, Metaxas G, et al. **Follow-up of intracranial aneurysms treated with stent-assisted coiling: comparison of contrast-enhanced MRA, time-of-flight MRA, and digital subtraction angiography.** *J Neuroradiol* 2017;44:44–51 CrossRef Medline